EurJOC
European Journal of Organic Chemistry

Full Papers
doi.org/10.1002/ejoc.202101080

Chemistry Europe
European Chemical Societies Publishing

Thioureidocalix[6]arenes Pseudorotaxanes

Gianpiero Cera,*[a] Margherita Bazzoni,[a] Leonardo Andreoni,[b, c] Federica Cester Bonati,[a] Chiara Massera,[a] Serena Silvi,*[b, c] Alberto Credi,[c, d] Andrea Secchi,[a] and Arturo Arduini*[a]

Dedicated to Prof. Vincenzo Balzani on the occasion of his 85th birthday

Heteroditopic calix[6]arenes are extensively exploited as synthetic receptors and as molecular components of supramolecular threaded and interlocked structures. We describe the synthesis of two novel calix[6]arene macrocycles, the upper rim of which is functionalized with either two or three phenylthioureido groups. These moieties are excellent hydrogen-bond donors and largely affect the conformation of the macrocycle, both in solution and in the solid state. Alternate conformers are observed in solution, and they give rise to supramolecular chains in the solid state. Moreover, and because of this conformational freedom, also the recognition properties toward the formation of pseudorotaxanes with bipyridinium-based axles are strongly affected. The number of phenylthioureido units of the macrocyclic host and the nature of the counterions of the bipyridinium guest determine the stability of the complexes. NMR, UV-Vis and electrochemical measurements revealed that very stable 1:1 inclusion complexes are formed between the triphenylthioureido calix[6]arene and a bipyridinium guest with tosylate counterions, whereas no complex is observed between the diphenylthioureido macrocycle and a hexafluorophosphate bipyridinium salt.

Introduction

Heteroditopic calix[6]arenes constitute an important class of macrocycles that has been extensively exploited to build synthetic receptors,[1] several stimuli-responsive devices and prototypes of molecular machines.[2] The modular nature of this supramolecular scaffold allows for its regioselective functionalization, leading to the synthesis of non-palindromic wheels, which are currently exploited to construct threaded complexes belonging to the family of (pseudo)rotaxanes.[3] This feature is made possible by a hydrogen-bonding donor (HBD) domain at the upper rim of the calixarene scaffold. Indeed, in low-polarity media, hydrogen-bonding interactions are able to separate the ion-pair of mono- and di-cationic (bi)pyridinium salts, promoting the unidirectional threading of these axles inside the π-rich aromatic cavity.[4]

This feature is of high importance in supramolecular chemistry because it allows for the design of linear molecular motors. In this context, the use of triphenylureido calix[6]arenes (**TPU**) is well-established (Figure 1 a).[3] It is a matter of fact that the nature and number of HBD – groups appended at the upper rim have an influence on the conformation of the macrocycle and the efficiency of anion-binding. As already mentioned, the complexation of the anions of the electron-accepting guest can govern the direction of threading, which is an important feature in the design of linear molecular motors. By playing with the nature and number of HBD moieties, we expect to influence the conformation and stability of the pseudorotaxane complex. To this end, we introduced a novel heteroditopic receptor, the diphenylureido calix[6]arene (**DPU**) which presents only two HBD moieties (Figure 1b).[5] This wheel, which in low-polarity solvents is present as a mixture of *1,2,3-alternate* (*1,2,3-alt*) and *cone* (*C*) conformations (≈4:1), is able to thread bipyridinium salts, and the threading process resulted in two different pseudorotaxane systems, P[**DPU**(*1,2,3-alt*)⊃DOV]2OTs and P[**DPU**(*C*)⊃DOV]2OTs (≈1:1), in solution (Figure 1). Very recently, our group succeeded to control the conformation of calix[6]arene-based pseudorotaxanes as a function of the counterion associated with the viologen salt. This was made possible with the synthesis of a novel family of heteroditopic wheels, which are characterized by three acidic NH sulfonamides (**TSA**) (Figure 1c).[6] Indeed, in the presence of tight ion pairs, the threading process led to the formation of a

[a] Prof. G. Cera, Dr. M. Bazzoni, F. Cester Bonati, Prof. C. Massera, Prof. A. Secchi, Prof. A. Arduini
Dipartimento di Scienze Chimiche, della Vita e della Sostenibilità Ambientale,
Università di Parma
Parco Area delle Scienze 17/A, 43124 Parma, Italy
E-mail: gianpiero.cera@unipr.it
arturo.arduini@unipr.it
[b] Dr. L. Andreoni, Prof. S. Silvi
Dipartimento di Chimica "G. Ciamician",
Università di Bologna
Via Selmi 2, 40126 Bologna, Italy
E-mail: serena.silvi@unibo.it
[c] Dr. L. Andreoni, Prof. S. Silvi, Prof. A. Credi
CLAN-Center for Light Activated Nanostructures,
Istituto per la Sintesi Organica e la Fotoreattività,
Consiglio Nazionale delle Ricerche
Via Gobetti 101, 40129 Bologna, Italy
[d] Prof. A. Credi
Dipartimento di Chimica Industriale "Toso Montanari",
Università di Bologna
Viale del Risorgimento 4, 40136 Bologna, Italy

Supporting information for this article is available on the WWW under https://doi.org/10.1002/ejoc.202101080

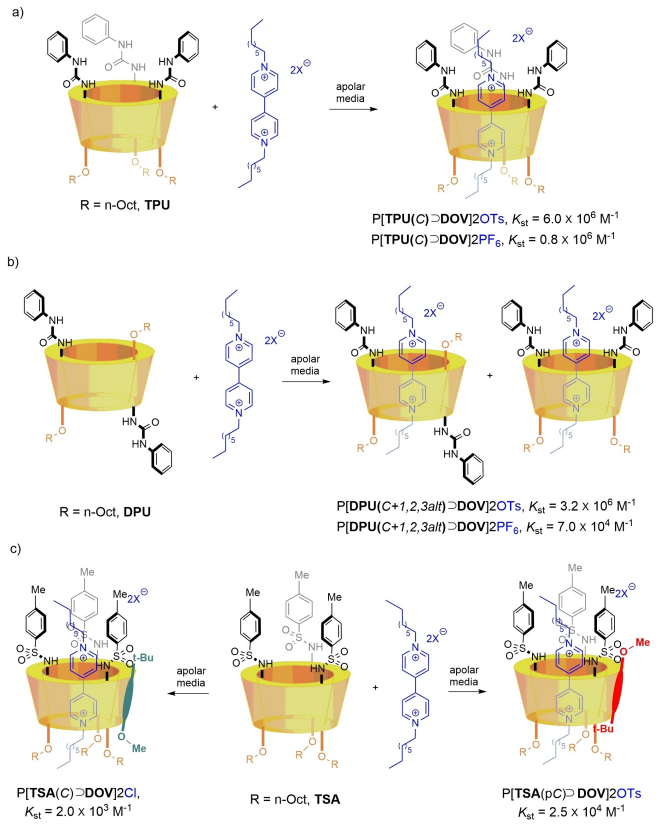

Figure 1. Key complexation features and association constants (K_{st}) of established calix[6]arene-based heteroditopic receptors.

pseudorotaxane with the calix[6]arene in a *partial cone* (pC) conformation. Contrarily, in the presence of weak ion pairs, pseudorotaxanes were formed in a typical *cone* conformation. These findings suggest that the number and the relative HBD ability of the functional groups at the upper rim of the calix[6] arene wheels might play an important role in promoting the threading process and controlling the conformation of the wheel in the resulting threaded species.

Thioureas are ubiquitous subunits in organic chemistry whose HBD ability is employed to design synthetic receptors[7] and catalysts.[8] It is noteworthy that thioureas can establish two-directional H-bonds with multidentate or spherical counterions. However, a significant difference with respect to their parent ureas subunits is represented by their inherently higher acidity (pK_a = 21.1 vs 26.9 in DMSO).[9] This property should result in more stable complexes with counterions, thus enhancing the stability of a host-guest complex.[10] Nevertheless, a counterintuitive outcome has been demonstrated when comparing urea vs thiourea as anion receptors:[11] indeed, the higher acidity of thiourea could result in anions protonation to the detriment of the supramolecular host-guest interaction. With these premises, we now introduce a new generation of heteroditopic calix[6]arene analogues substituted with thioureido groups.[12] Within this study, we aim to analyze how the increased HBD ability of supramolecular wheels could impact the complexation ability of calix[6]arenes in forming pseudorotaxane-based assemblies.

Results and Discussion

Synthesis

At the outset of the investigation, we synthesized two novel thiourea-based calix[6]arene wheels. Notably, triphenylthioureido calix[6]arene **TPT** differs from a previously reported thioureido analogue by the R group (*n*-octyl instead of ethoxyethyl, see Scheme 1).[12] We started from the known trioctyloxytrinitro (**TN**)[13] and dioctyloxydinitro (**DN**) derivatives.[5] Reduction of the nitro groups with hydrazine, in the presence of catalytic amounts of Pd/C (10 mol%), led to the corresponding tri- and di-amino intermediates, which were then reacted with an excess of phenylisothiocyanate, in CH_2Cl_2 at room temperature. Hence, triphenylthioureido (**TPT**) and diphenylthioureido (**DPT**) calix[6]arenes were obtained in good yields (87% and 82%, respectively) (Scheme 1).

Subsequently, we investigated the conformations of the newly devised thioureido calix[6]arenes by ^{1}H-NMR spectroscopy. Particularly, in low-polarity solvents, **TPT** adopts, on the NMR time-scale, a *pseudo cone* conformation. This geometry was unambiguously confirmed by variable temperature NMR spectroscopy using tetrachloroethane-d_2 as the solvent. Indeed, at 373 K, **TPT** presents an AX system of two doublets at 4.5 and 3.6 ppm (^2J = 15.4 Hz), related to the bridging axial and equatorial methylene groups of the macrocycle and a broad singlet at 2.6 ppm for the three methoxy groups which point towards the center of the cavity (Figure 2 and Supporting

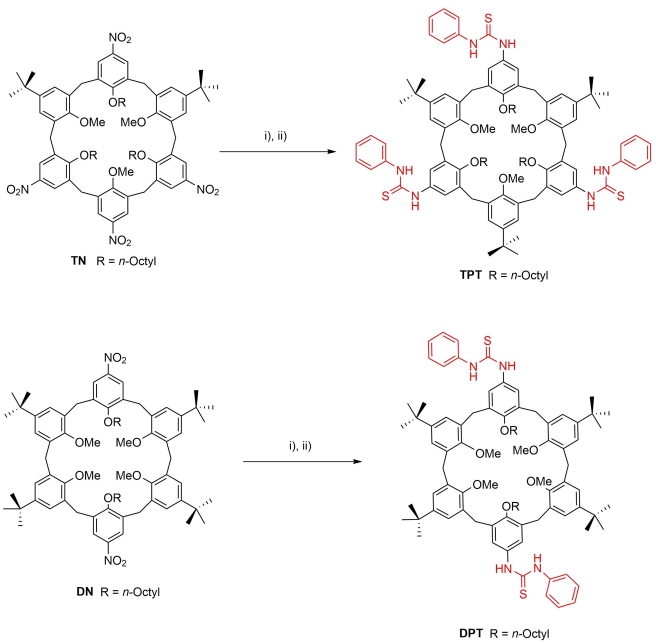

Scheme 1. Synthesis of thioureido calix[6]arenes **TPT** and **DPT**: i) Pd/C (cat.), $N_2H_4 \cdot H_2O$, EtOH, reflux, quant.; ii) PhNCS, CH_2Cl_2, 25 °C.

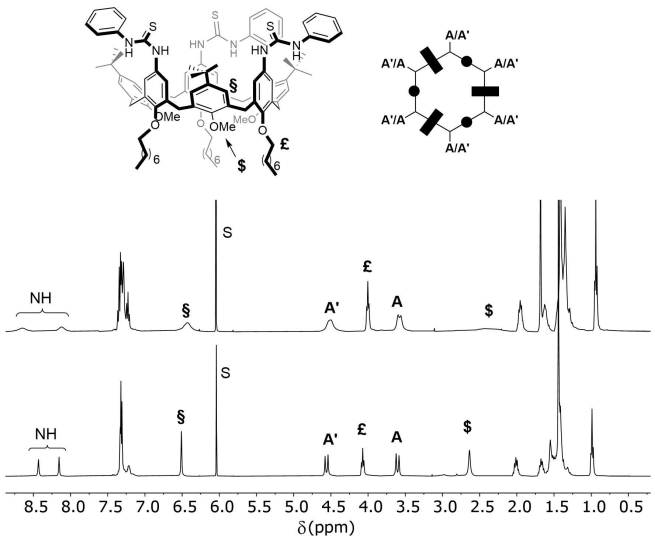

Figure 2. Stacked plot ^{1}H-NMR (tetrachloroethane-d_2) of **TPT** at 298 K (top) and 373 K (bottom).

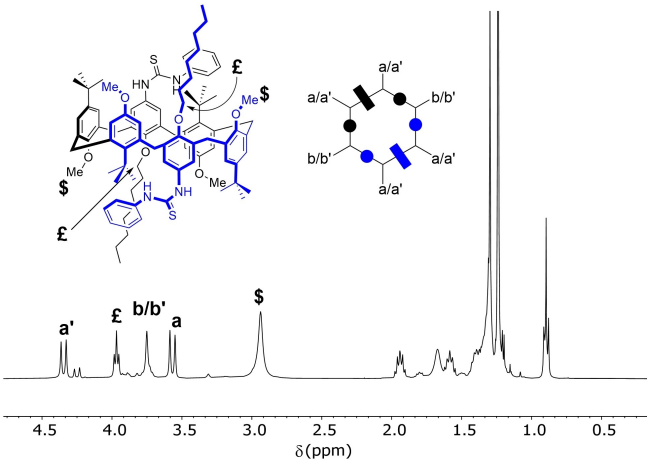

Figure 3. Upfield expanded region of the ^{1}H NMR spectrum (400 MHz, 298 K) of **DPT** in $CDCl_3$. At the top are schematic representations of **DPT**. The rectangle identifies the phenolic ring substituted with the octyloxy chains, while the circle identifies those with methoxy groups.

Information). Finally, the *anti/syn* conformation of thioureido moieties[14] in nonpolar media was established by selective ROESY experiments (see Supporting Information).

As expected, a different situation was observed for the di-substituted thioureido derivative. In fact, ^{1}H-NMR analysis in $CDCl_3$ at 298 K, revealed that, analogously to **DPU**, **DPT** is mainly present as a *1,2,3-alternate* conformer.[13,15] The most notable features of ^{1}H-NMR for **DPT** include a single, broad peak at 2.92 ppm related to the four symmetric methoxy groups ($) of the calix[6]arene unit. Furthermore, a new pattern was observed for the methylene bridging protons. Particularly, we detected two doublets at 4.3 and 3.6 ppm with a geminal coupling of $^2J = 14.8$ Hz for the a/a′ couple. Interestingly, a singlet at 3.75 ppm for the b/b′ couple, typical of an *anti*-orientation, suggested a single inversion point (Figure 3). ^{1}H- and HSQC NMR spectra carried out at higher temperatures (313-328 K) showed four doublets, with geminal coupling, two for the axial and two for the equatorial protons in a 2:1:1:2 ratio for the minor conformation (see SI). This outcome, similar to the one found for its phenylureido analogue **DPU**, led us to finally attribute to this minor specie, a *pseudo cone* conformation (*1,2,3-alt* vs *pseudo cone* ≈4:1). The presence of these major conformers in slow exchange was finally confirmed by variable temperature NMR analysis (see SI).

X-ray crystal structures

Intrigued by the high selectivity towards the formation of a *1,2,3-alternate* conformer, major efforts were directed toward the crystallization of **DPT** to verify whether the preorganization of the thioureido groups could influence the structure of the macrocycle in the solid-state as well. The crystal structure of compound **DPT** was determined *via* X-ray diffraction data on single crystals obtained by slow evaporation of a $CHCl_3$/methanol solution. The asymmetric unit comprises two independent half molecules and a crystallization methanol molecule that could not be sensibly modelled and whose electron density was hence removed (see the experimental part for the details). Figure 4 shows the molecular structure of the two independent **DPT** calix[6]arenes **I** and **II**, respectively; they both show a *1,2,3-alternate* conformation with three independent aromatic rings forming the walls of the cavity labelled A, B, C (**I**) and D, E, F (**II**). With respect to the mean plane passing through the six methylene bridges of the lower rim, the mean planes passing through the aromatic rings are inclined of 75.1(3), 64.3(4), 42.1(3), 79.6(4), 39.5(2) and 71.2(2)° for A, B, C (**I**) and D, E, F (**II**), respectively (the values reported are those smaller than 90°).

In each calixarene, two symmetry-equivalent methoxy groups point inside the cavity, namely O1C–C8C (**I**) and O1E–C8E (**II**), which form C–H···π interactions with the aromatic walls [C8C–H8C3···C6A, 3.355(2) Å and 127.5(3)°; C8E–H8E3···C6D, 3.363(2) Å and 126.7(4)°, see Supporting Information]. The position of the phenylthioureido arm is

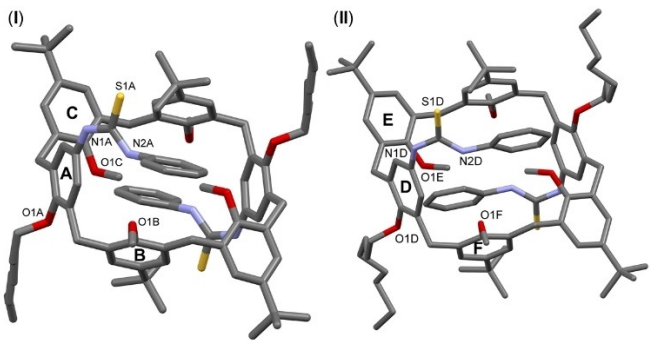

Figure 4. Molecular structures of **I** and **II** with partial labeling scheme for the atoms in the asymmetric unit. Hydrogen atoms and solvent molecules have been omitted for clarity. The symmetry code to generate the whole molecule is 2-x, 1-y, 1-z and 1-x, -y, 2-z for **I** and **II**, respectively.

different in **I** and **II**. In **I**, a weak hydrogen bond is formed between the N2A–H2N moiety and the methoxy oxygen atom O1B [N2A–H2N···O1B, 3.157(1) Å and 125.9(1)°, see SI]. Besides, the phenyl group attached to N2 A is inclined of 32.9(3)° with respect to the mean plane passing through the methylene bridges. In **II**, a weak interaction exists between the C19D–H19D group of the phenyl ring and the oxygen atom O1E of the methoxy group [C19D–H19D···O1E, 3.300(1) Å and 135.4(1)°, see SI]. Differently from **I**, the phenyl ring attached to N2D is inclined of 67.1(4)° with respect to the mean plane passing through the methylene bridges. In the lattice, the two molecules **I** and **II** are connected through H bonds involving the thioureido groups, with the N–H atoms behaving as donors and the sulfur atoms as acceptors [N1A–H1N···S1D, 3.497(2) Å and 170.6(1)°; N1D–H3N···S1A, 3.231(1) Å and 145.5(1)°]. This motif connects symmetry-related molecules **I** and **II** in a supramolecular chain parallel to the plane (101) (Figure 5). The overall packing in the three dimensions is dominated by dispersion interactions.

NMR characterization of the complexes

Having now at our disposal more information regarding the nature and the electronic properties of thioureido substituted hosts, we evaluated how these features affect their ability to work as supramolecular receptors for dicationic bipyridinium-based axles. Towards this end, we first equilibrated a solution of **TPT** (18 mM) with the tosylate salt of 1,1′-dioctyl-4,4′-bipyridinium (DOV·2OTs) at 298 K (1:1 in $CDCl_3$). Hence, a deep red solution was obtained and subsequently analyzed by NMR spectroscopy. At first glance, we observed the formation of two different pseudorotaxane species in solution in a 2:1 ratio (Scheme 2). This was confirmed by the upfield shift of the aromatic CH and N–CH_2 peaks of the guest and their eventual splitting in two sets of signals. A similar trend was observed for methoxy groups as well. Particularly, a downfield shift of the methoxy groups ($\Delta\delta = 1.5$) gave rise to three different signals. A broad singlet (**$**$^{\#}$), which is related to the major *cone* conformer P[**TPT**(*C*)⊃DOV]2OTs, and two further singlets, in a 2:1 ratio (**$*** and **£***), are suggestive of a minor pseudorotaxane species in which the wheel lost its inherent symmetry. In this threaded structure, the two doublets (ax + eq) A/A′ of the methylene bridge in **TPT** split into six doublets, with geminal coupling, in a 1:1 ratio. The HSQC spectrum (see SI) revealed a significant shift of the ^{13}C resonances for the α/α' couple to $\delta = 35.6$ ppm, suggesting a single inversion point. Further investigation led us to associate this inversion to a ring bearing a methoxy group, yielding a pseudorotaxane P[**TPT**(p*C*)⊃DOV]2OTs in which the host adopts a *partial cone* conformation (p*C*). This finding is quite interesting compared to the reactivity of triphenylureido analogues in the presence of tight ion pairs. It is noteworthy that **TPU** is able to selectively form pseudorotaxanes, with the host adopting a *cone* conformation (see Figure 1a). This parallel seems to suggest that the enhanced HBD ability of the **TPT** system could be related to a slight, yet notable, shift in the selectivity (*cone* vs *partial cone*) associated to the formation of pseudorotaxane-based systems in analogy to what we have recently disclosed for **TSA** calix[6]arenes (see SI).[6]

A variable temperature NMR experiment was carried out on a solution of P[**TPT**⊃DOV]2OTs in tetrachloroethane-d_2 (see SI) to establish whether the **TPT** conformational interconversion may occur also after the complexation reaction. As expected, a temperature increase induces a higher fluxionality of both the macrocycle and the thread but without appreciably affecting the stability of the pseudorotaxane complex. At 373 K, the coalescence conditions were not observed yet and, although very broad, the resonances belonging to P[**TPT**(*C*)⊃DOV]2OTs and P[**TPT**(p*C*)⊃DOV]2OTs were still recognizable. This non conclusive VT experiment seems, however, to show that *i*) once the wheel/axle adduct is formed, the p*C*-to-*C* interconversion requires the overcoming of a rather high energy barrier, and *ii*) the formation of the pseudorotaxane complex with the wheel adopting the *partial cone* conformation is likely guided by the formation of HB between the thiourea moieties and the axle counteranions (see also computational studies).

To evaluate the role of the counterion on the complexation ability of **TPT**, we next performed NMR studies using DOV·2PF_6 as a guest (1:1 in $CDCl_3$). Analysis of the ^{1}H-NMR spectrum revealed only a poor formation of any pseudorotaxane species. This could be rationalized in terms of weak coordination abilities of the PF_6 counterion, which is not able to promote an efficient rearrangement of the thioureido moieties to the binding-active *anti/anti* conformation.[16] To get more insights, increasing amounts of tetrabutylammonium tosylate salt, TBAOTs, (up to 3 equivalents) were added to the mixture to exchange PF_6 anions present in solution. Thus, a typical NMR pattern as previously observed for P[**TPT**⊃DOV]2OTs highlighted the importance of tight coordinating counterions to promote the threading of bipyridinium salts inside the π-rich aromatic cavity of **TPT** (see SI).

We next attempted a study on the complexation ability of **DPT** by mixing a solution of this compound with DOV·2OTs. ^{1}H-NMR analysis disclosed an even more complicated outcome. The "free" **DPT** in the *1,2,3-alt* conformation is the most abundant species in solution. However, the appearance of a down-fielded resonance for the methoxy groups along with the presence of four up-field shifted resonances for the aromatic CH bonds of the bipyridinium suggested the formation of the corresponding pseudorotaxane P[**DPT**⊃DOV]2OTs (see SI). This scenario led us to propose that the binding properties of **DPT**, at the NMR time-scale, are highly influenced by the formation of HB aggregates also in solution. Several experiments were carried out in order to solve the riddle. At first, HB-competition experiments were performed adding increasing amounts of a polar protic solvent such as methanol-d_4 to a mixture of **DPT** in $CDCl_3$.[17]

The analysis of the ^{1}H-NMR stack plot depicted in Figure 6 revealed a progressive broadening of the calixarene resonances as the amount of the polar solvent added increased.[18] More interestingly, a splitting of the doublets previously assigned to the bridging methylene groups of **DPT** in the *cone* and *1,2,3-alternate* conformation was observed (see e.g. inset of Figure 6). For the same reason, an upfield shifting broad resonance (●)

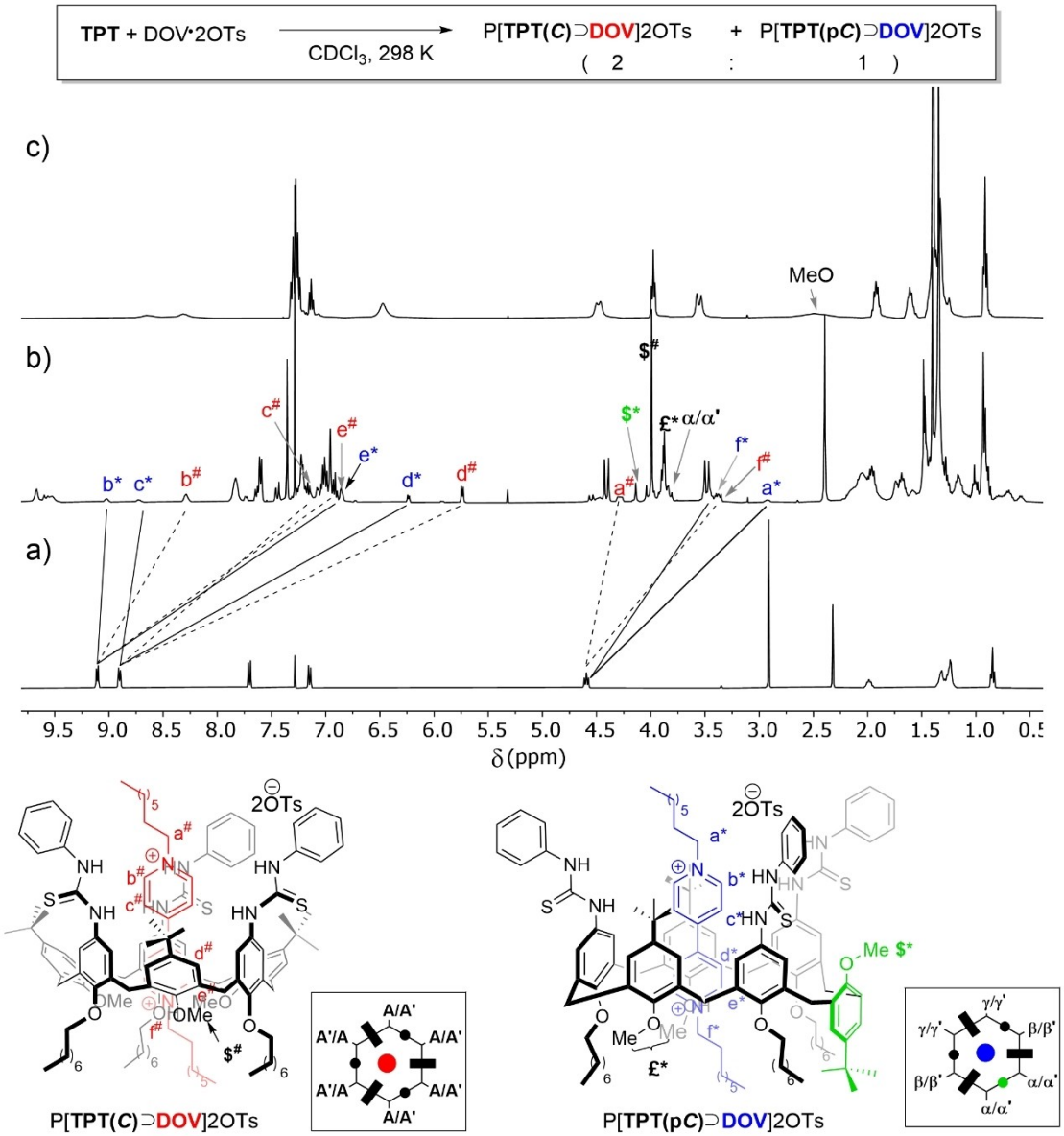

Scheme 2. [1]H-NMR spectra (400 MHz, 298 K) of a) DOV·2OTs in CD_3CN, b) pseudorotaxane P[**TPT**(*C*+p*C*)⊃DOV]2OTs in $CDCl_3$, c) **TPT** in $CDCl_3$. Bottom, schematic representation P[**TPT**(*C*)⊃DOV]2OTs and P[**TPT**(p*C*)⊃DOV]2OTs and the assignment of proton resonances. The color of the ovals/rectangles shows the relative position of the phenolic substituent with respect to the plane defined by the bridging methylene groups (hexagon), i.e. black upward, green downward. The rectangle identifies the phenolic rings substituted with the octyloxy chains, while the circle those with the methoxy group.

appears beside the original methoxy resonances at 2.92 ppm (○). Thus, some DOSY NMR experiments[19] were carried out on solutions of **DPT** in neat $CDCl_3$ and in a 5% v/v $CD_3OD/CDCl_3$ mixture (see SI). For the latter solution, the mono-exponential fitting of the intensity decay of the two methoxy resonances (○) and (●) as a function of the gradient strength *G* (see SI) yielded a diffusion coefficient *D* of 4.76 and 5.60×10^{-10} m^2s^{-1}, respectively. It is noteworthy to observe that the diffusion coefficient calculated by fitting the decay of the unique methoxy resonance (○) present in the spectrum of **DPT** in neat $CDCl_3$ matched the one calculated for the minor component of the mixture of Figure 6d (4.75 vs. 4.76). The results of the DOSY experiments are difficult to rationalize when the diffusing species in solution result from an isodesmic self-assembly process,[20] which gives rise to a distribution of aggregates of different size. In our case, this was further complicated by the extensive overlapping of the aggregates resonances (see SI) that, worsening the peaks fitting, allows only to determine average diffusion coefficients. To avoid any misinterpretation of the above diffusion NMR experiment, we also performed some DLS measurements to verify the presence of the aggregates in chloroform solution. A first analysis was carried out on a 7 mM solution of **DPT** and showed a unique major specie (see SI). Interestingly, when MeOH was added to this solution, we observed the formation of new species with diminished averaged sizes. Although just qualitative, these findings

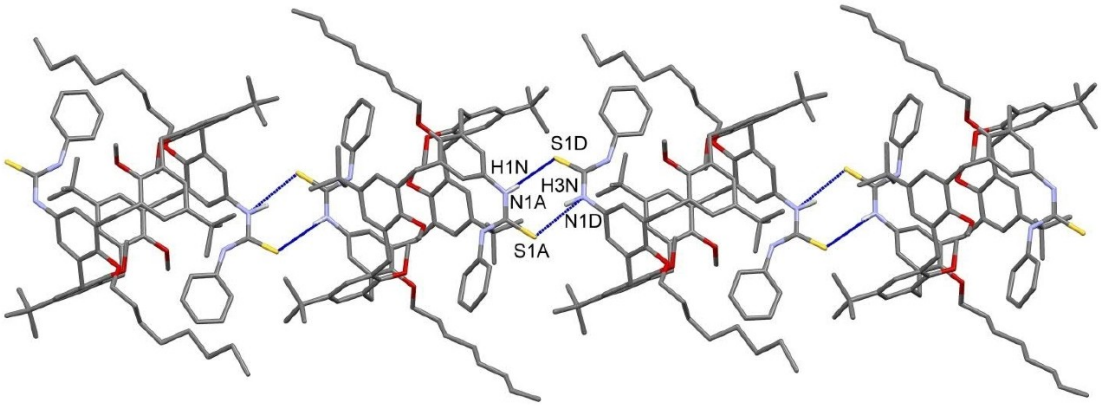

Figure 5. The set of H-bonds involving the two independent molecules **I** and **II** forming chains parallel to (101). Hydrogen atoms not involved in the interactions have been omitted for clarity. H bonds are shown as blue lines.

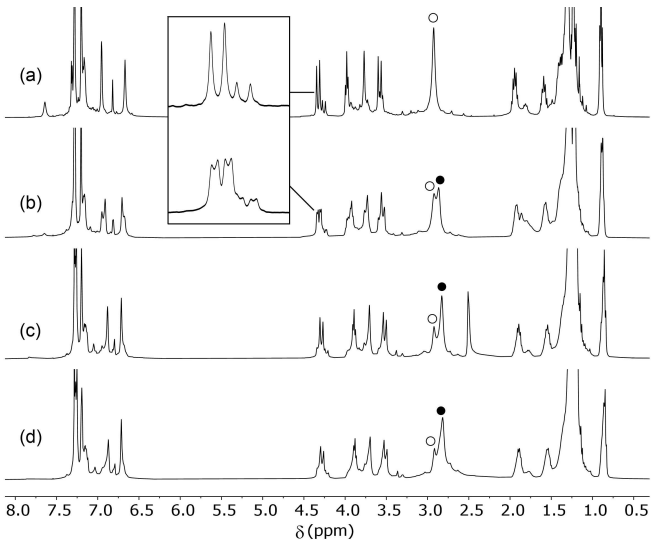

Figure 6. ^{1}H NMR stack plot (400 MHz) recorded upon addition of increasing amount of CD_3OD (b–d, up to a 5% v/v of CD_3OD) to a solution of (a) **DPT** in neat $CDCl_3$ at $T = 298$ K. In the inset, a magnification of the splitting endured by the resonances of the host bridging methylene protons upon methanol addition is presented. The symbols (○) and (●) show the methoxy resonances of the most abundant aggregates present in the solution containing methanol.

advocate for the presence in chloroform solution of self-assembled species in agreement with what found in the solid state (see Figure 5).

Computational studies

To disclose the role of the conformation adopted by **TPT** in the pseudorotaxane stabilization, the structure of the two interwoven complexes P[**TPT**(*C*)⊃DOV]2OTs and P[**TPT**(p*C*)⊃DOV]2OTs was optimized through semiempirical quantum-chemical methods. We used the PM6-DH+ method,[21] implemented in the Mopac 2016 program,[22] using the COSMO implicit solvation model to simulate the chloroform media. Indeed, this method implements empirical corrections for dispersion and hydrogen-bonding interactions and we have shown it performs well in modelling similar pseudorotaxane systems based on **TSA** calix[6]arenes.[6] As expected, the optimized geometry of both complexes shows that the two tosylate anions are H-bonded with the host thioureido moieties (Figure 7a–d). A tosylate anion, with two of its oxygens, is engaged in four HBs with four NHs of two convergent phenylthioureas. The other tosylate is H-bonded, using two oxygens, to the remnant thiourea. Its third oxygen sits in proximity of the electron poor pyridinium ring of DOV emerging from the calix[6]arene cavity. The difference of heat of formation (HoF) calculated for the two pseudorotaxanes (≅5 kcal/mol, see Figure 7) could explain the preferential formation of P[**TPT**(*C*)⊃DOV]2OTs with respect to P[**TPT**(p*C*)⊃DOV]2OTs found through the previous NMR studies (*C*:p*C*≅2:1).[23]

With regard to the free **TPT**, some structural guesses in which this host can adopt either a *cone* or a *partial cone* conformation with the thiourea moieties in *syn/anti* and *anti/anti* configuration were minimized. The calculated HoF in chloroform evidences that the *syn/anti* configuration is the preferred one in both the calix[6]arene conformers (see SI). Interesting findings were obtained for **DPT**, as well (Figure 7e, Figure 7f). Here, the *syn/anti* arrangement of the NHCSNH moieties promotes the formation of intramolecular H-bonding between a *syn* NH of thiourea and one OMe group of the anisole moieties (purple arrows, Figure 7e, Figure 7f). This type of intramolecular H-bonding, also observed in the solid state (see SI), forces the phenylthiourea units on the calix[6]arene wider rim to close the cavity access of **DPT**. This evidence supports once more that the threading abilities of **DPT** are highly influenced by secondary inter- and intramolecular interactions.

UV-Vis and electrochemical characterization

The association of the two thioureido calix[6]arenes with DOV·2OTs and DOV·2PF_6 was investigated by UV-Vis spectro-

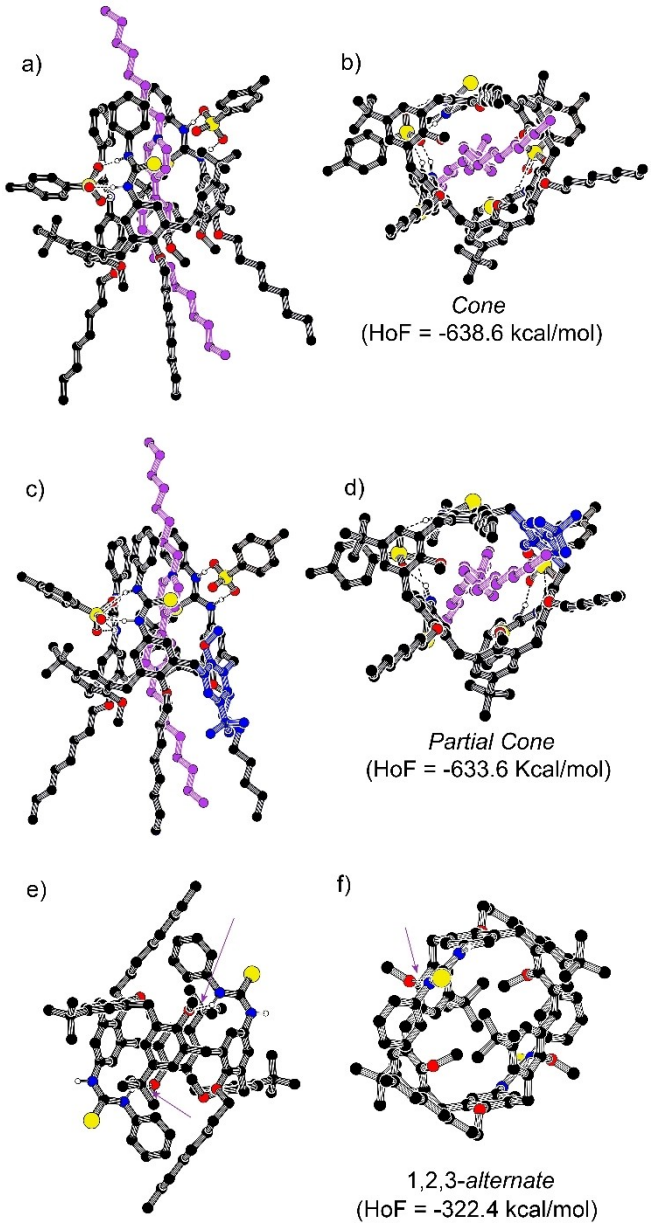

Figure 7. Side and top pluton views of the optimized geometry (PM6-DH+) of pseudorotaxanes P[**TPT**(*C*)⊃DOV]2OTs (a–b) and P[**TPT**(p*C*)⊃DOV]2OTs (c–d) and **DPT** (e–f). For better clarity, the backbones of the dioctylviologen threads are colored in purple; all hydrogen atoms except those taking part in H-bonding have been omitted, and the "flipped" aromatic ring of the *partial cone* conformation in panels c and d are highlighted in a light blue color. Colors: C, black; N, blue; O, red; H, white; S, yellow; H-bonds, dashed black lines.

scopy. The absorption spectra of **TPT** and **DPT** are characterized by a strong absorption band in UV, at $\lambda_{max}=269$ nm and 277 nm with $\varepsilon=45000\ M^{-1}cm^{-1}$ and $41000\ M^{-1}cm^{-1}$, respectively. The shift on λ_{max} might be related to the number of different conformations that **DPT** or **DPU** assume in the solution. By comparing the absorption spectrum of an equimolar mixture of **TPT** and DOV·2OTs with the sum of the spectra of the separated components, a red shift of the main UV band is observed, together with the appearance of a weak band in the visible region, which is usually ascribed to the charge transfer interaction between the electron donor macrocycle and the electron accepting guest (Figure 8). Two differences can be highlighted with respect to the parent **TPU**-based pseudorotaxanes: first, the absorption change in the UV region upon complexation is much less pronounced for the **TPT** complex with respect to the **TPU** one; besides, the charge-transfer band is shifted toward higher energies ($\lambda_{max}=410$ nm vs $\lambda_{max}=460$ nm) and is more intense ($\varepsilon=800\ M^{-1}cm^{-1}$ vs $\varepsilon=500\ M^{-1}cm^{-1}$). These observations could be ascribed to the differences in the nature of the HBD units and in the conformations of the final complexes, as evidenced also by NMR experiments.

Spectrophotometric titrations were performed (Figure 8) and the apparent stability constant determined by fitting the data with a 1:1 binding model is $1.2\times10^{7}\ M^{-1}$. This large association constant is comparable with the values obtained for similar pseudorotaxanes formed by **TPU** and bipyridinium-based axles with tosylate counterions.[24] Similar spectroscopic changes were observed upon investigation of the complexation of **DPT** with DOV·2OTs, with an association constant of $3.0\times10^{4}\ M^{-1}$. This value is three and two orders of magnitude smaller with respect to the analogous pseudorotaxanes formed with **TPT** and **DPU**, respectively. Indeed, also NMR experiments suggest a more complicated picture for this host-guest complex, most likely related to the different conformations assumed by the **DPT** receptor and/or to the competitive intramolecular HB interactions between the thioureido groups, which might promote the formation of clusters both in solution and at the solid state. As suggested by NMR experiments, only slight or no changes in the absorption spectra were observed upon mixing **TPT** and **DPT** with DOV·2PF_6, respectively (see SI). To confirm the influence of the nature of the counterions on the binding abilities of both **TPT** and **DPT**, anion exchange experiments were performed, by adding tetrabutylammonium salts with tosylate or hexafluorophosphate anions to the preformed mixtures of axles and wheels. Indeed, addition of

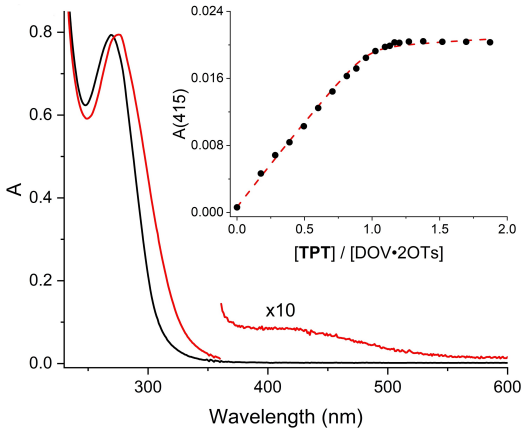

Figure 8. Sum of the absorption spectra (black line) and the absorption spectrum of the mixture (red line) of CH_2Cl_2 solutions of DOV·2OTs (1.4×10^{-5} M) with **TPT** (1.2×10^{-5} M). The inset shows the titration curve (black dots) together with the fitting of the data (dashed line).

increasing amounts of TBAOTs to a 1:1 mixture of **TPT** and DOV·2PF$_6$, up to 2 equivalents, caused the characteristic absorption changes related to the formation of the pseudorotaxane complex, i.e., a red shift of the UV band and the appearance of the CT band. On the contrary, upon addition of TBAPF$_6$ to P[**TPT**(*C*)⊃DOV]2OTs and P[**DPT**(*C*)⊃DOV]2OTs up to 100 equivalents, a decrease in the CT bands was observed. These results clearly suggest a strong influence of both the counterions of the guest and the nature and number of HBD donor groups of the host on the stability of the pseudorotaxane complexes.

The pseudorotaxanes formed between the two thioureido calix[6]arenes with DOV·2OTs were investigated by cyclic voltammetry (CV) and differential pulse voltammetry (DPV) in CH_2Cl_2. On consideration of the strong effect of the anions on the stability of the pseudorotaxanes, TBAOTs was used as supporting electrolyte. The bipyridinium guest is characterized by two monoelectronic and reversible reduction processes, at −0.42 and −0.86 V (vs SCE, Figure 9).[25] It is worth noting that the tosylate anion affects the first reduction potential of the bipyridinium ion (the first reduction process for DOV·2PF$_6$ being at −0.29 V *vs* SCE)[24] . This effect can be related most likely to the formation of a strong ion pair between tosylate anions and the bipyridinium dication, which is then more difficult to reduce.[25c] Both pseudorotaxanes follow the same electrochemical behavior of parent compounds based on phenylureido calix[6]arene hosts, i.e., dissociation occurs upon reduction of DOV·2OTs. Indeed, the first reduction process is shifted to more negative potential values (E = −0.74 V vs SCE, from DPV measurements) and it is almost superimposed to the second process (Figure 9), on account of the host-guest charge transfer interaction. The second reduction process, though, occurs at the same potential value of the free bipyridinium radical cation, thus confirming that the monoreduced axle dethreads from the calix[6]arene host. Upon reoxidation, the two anodic waves of the free bipyridinium are observed.

Spectroscopic and electrochemical data suggest that the charge transfer interaction in **TPT**- and **DPT**-based pseudorotaxanes is comparable: indeed the energy of the CT band and the shift of the potential of the encapsulated guest are similar in the two complexes. On the other hand, titration experiments demonstrate that P[**TPT**(*C*)⊃DOV]2OTs is more stable than P[**DPT**(*C*)⊃DOV]2OTs, whereas the analogous complexes with DOV·2PF$_6$ do not form at all. These results, taken together and compared with the results on parent **TPU**- and **DPU**-based pseudorotaxanes, highlight that the stability of these complexes is not only related to the charge transfer interaction, but the nature and number of HBD donors on the host, and the nature of the anions of the guest have a strong influence on the host-guest complex.

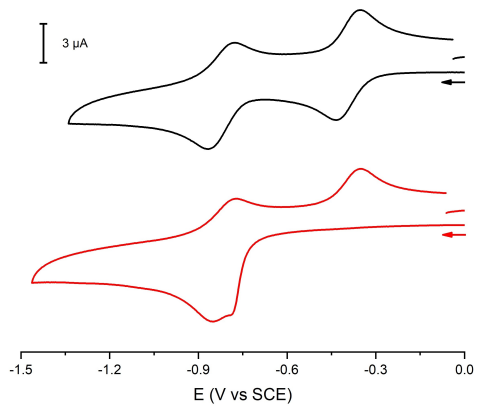

Figure 9. Cyclic voltammograms of DOV·2OTs (black line) and P[**TPT**(C)⊃DOV]2OTs (red line) in CH_2Cl_2 at room temperature ([DOV·2OTs] = 1.5×10^{-4} M, [**TPT**] = 1.8×10^{-4} M, 100-fold TBAOTs, scan rate: 200 mV/s).

The lower stability of P[**DPT**(*C*)⊃DOV]2OTs with respect to P[**TPT**(*C*)⊃DOV]2OTs can be qualitatively justified on the basis of the lower number of HBD units. On the other hand, though, the lower stability of P[**DPT**(*C*)⊃DOV]2OTs with respect to P[**DPU**(*C*)⊃DOV] 2OTs[5] is counterintuitive, on the sole basis of the nature of the HBD units. Indeed, as suggested by NMR experiments, **DPT** is mainly present in a *1,2,3-alternate* conformation, which is not preorganized to host the bipyridinium guest inside its cavity. Moreover, this observation could also be rationalized in terms of competitive intra- and intermolecular HB interactions between the thioureido groups that might promote the formation of clusters both in solution and in the solid state. This propensity of the thioureido units to form intra- and intermolecular interactions could be also at the basis of the lack of association with DOV·2PF$_6$. Indeed, the HBD units on the calix[6]arene have also a structural role, as they can confer the correct *cone* conformation, preorganizing the wheel to include the guest. Overall, the formation of the supramolecular complex results from several competing equilibria: ion-pairing between the bipyridinium ion and its counterions; charge-transfer interaction between the electron donor cavity of the host and the electron acceptor guest; hydrogen bonding between the HBD groups of the host and the counterions of the guest; intramolecular interactions between the HBD groups of the host, which may also affect the conformation and preorganization of the macrocycle.

Conclusion

We reported the synthesis of two novel tri- and dithioureido calix[6]arene derivatives (**TPT** and **DPT**), able to form threaded complexes with bipyridinium-based dicationic axles, in solution. By means of NMR investigations, solid-state structure analysis and spectrophotometric titrations, we demonstrated how hydrogen bonding interactions impact the complexation features of these compounds. Nevertheless, when compared with phenylureido-functionalized calix[6]arenes, the behavior of **TPT** and **DPT** cannot be easily rationalized, both as a function of the number of the HBD groups and of the nature of the counterions of the guest. The association of **TPT** with DOV·2OTs is comparable with that of **TPU**, whereas **DPT** forms a much less stable complex as compared with parent **DPU**. An even stronger effect is observed when comparing the association of **TPU** and **TPT** with DOV·2PF$_6$: while the former forms a stable pseudorotaxane, the inclusion complex between **TPT** and

$DOV \cdot 2PF_6$ could hardly be detected by our techniques. These differences cannot be directly related to stronger hydrogen bonding abilities of **TPT** and **DPT**, which, actually, would lead to opposite outcomes. However, NMR experiments and solid-state structure analysis point out that the thioureido groups affect the conformation and preorganization of the macrocycles, especially with **DPT**. Alternate geometries or intermolecular interactions prevent molecular recognition: competition between these interactions and anion recognition is responsible of the final outcome. Apparently, the fortunate combination of phenylurea units and tosylate anions maximizes the stabilization of the pseudorotaxane. These results confirm once more how complex is the correlation of parameters that influence the supramolecular interaction and how challenging is to predict the structure and stability of the host-guest complexes. Moreover, these studies pave the way to future developments devoted to get more insights in the supramolecular forces that govern the conformational rearrangement of heteroditopic calix[6]arene hosts and to exploit the reactivity of **DPT** to construct pre-organized supramolecular structures such as organic polymers and nanowires.[26]

It is worth recalling here that the two different rims of calixarene macrocycles enable to control also the threading direction of the guest inside the cavity, an important feature to design molecular machines and motors. Indeed, it has been demonstrated that **TPU** is able to direct the insertion of tosylate bipyridinium axles exclusively from its upper rim in nonpolar solvents. More investigations will be devoted to unravelling the influence of the anions and anion receptors on the stability, conformation and dynamics of the supramolecular structures.

Experimental Section

Solvents were dried following standard procedures; all other reagents were of reagent grade quality, obtained from commercial sources and used without further purification. Chemical shifts are expressed in ppm using the residual solvent signal as an internal reference. Mass spectra were determined in ESI mode. **TN**[13] and **DN**,[5] axle DOV ditosylate[4c] were synthesized according to reported procedures. The synthesis of **DPT** and **TPT** was accomplished by slightly modifying previously reported protocols for **DPU** and **TPU**.[5,13]

Synthesis

TPT: In a two-neck flask kept under inert atmosphere, to a solution of **TN** (0.3 g, 0.22 mmol) in ethanol (100 mL), hydrazine monohydrate (1.0 g, 13 mmol) and a tip of spatula of 10% Pd/C catalyst were added. The resulting mixture was refluxed for 24 h and then filtered, still warm and under an inert atmosphere, through a celite pad to remove the palladium catalyst. The filtered solution was evaporated to dryness under reduced pressure. The residue was diluted in dichloromethane (50 mL), and the resulting organic phase was washed thrice with water to remove the excess of hydrazine. The separated organic phase was dried over anhydrous $CaCl_2$, filtered and evaporated to dryness under reduced pressure. The residue was dissolved in anhydrous dichloromethane (30 mL) and placed in a two-neck flask kept under an inert atmosphere. To the resulting homogeneous solution, phenyl isothiocyanate (0.1 g, 0.7 mmol) was added. The reaction mixture was stirred at room temperature for 24 h then the solvent was removed under reduced pressure. Purification by column-chromatography of the crude mixture (*n*-Hex: EtOAc = 8:2) afforded **TPT** in 82% yield as a white solid. M. p. = 130–133 °C. ^{1}H NMR (400 MHz, $CDCl_3$) δ = 8.65 (br.s, 3H), 8.21 (br.s, 3H), 7.39–6.99 (m, 21H), 6.45 (br.s, 6H), 4.63–4.23 (m, 6H), 3.97 (t, J = 7.8 Hz, 6H), 3.55 (d, J = 14.7 Hz, 6H), 2.83–2.08 (br.s, 6H), 1.99–1.81 (m, 6H), 1.67–1.51 (m, 6H), 1.45–1.08 (m, 57H), 0.94–0.86 (m, 9H). ^{13}C NMR (101 MHz, $CDCl_3$) δ = 179.7 (C_q), 154.5 (C_q), 153.8 (C_q), 146.6 (C_q), 137.9 (C_q), 136.6 (C_q), 132.9 (C_q), 132.6 (C_q), 128.9 (CH), 127.9 (CH), 126.2 (CH), 125.9 (CH), 124.6 (CH), 73.1 (CH_2), 60.9 (CH_3), 34.3 (C_q), 31.9 (CH_2), 31.6 (CH_3), 30.7 (CH_2), 30.5 (CH_2), 29.6 (CH_2), 29.3 (CH_2), 26.3 (CH_2), 22.7 (CH_2), 14.1 (CH_3). HR-MS (ESI) m/z: = $[M+H]^+$ calcd. for $C_{102}H_{133}N_6O_6S_3$: 1633.9449 found 1633.9442.

DPT: In a two-neck flask kept under inert atmosphere, to a solution of **DN** (0.7 g, 0.57 mmol) in ethanol (150 mL), hydrazine monohydrate (1.42 g, 28 mmol) and a tip of spatula of 10% Pd/C catalyst were added. The resulting mixture was refluxed for 48 h and then filtered, still warm and under an inert atmosphere, through a celite pad to remove the palladium catalyst. The filtered solution was evaporated to dryness under reduced pressure. The residue was diluted in dichloromethane (50 mL), and the resulting organic phase was washed thrice with water to remove the excess of hydrazine. The separated organic phase was dried over anhydrous $CaCl_2$, filtered and evaporated to dryness under reduced pressure. The residue was dissolved in anhydrous dichloromethane (50 mL) and placed in a two-neck flask kept under an inert atmosphere. To the resulting homogeneous solution, phenyl isothiocyanate (0.18 g, 1.4 mmol) was added. The reaction mixture was stirred at room temperature for 24 h then the solvent was removed under reduced pressure. Crystallization of the crude mixture from EtOAc afforded DPT in 87% yield as a white solid. M. p. = 194–196 °C. ^{1}H NMR (400 MHz, $CDCl_3$) δ = 7.35–7.13 (m, 18 H), 6.95 (br.s, 3H), 6.81 (br.s, 1H), 6.67 (br.s, 3H), 4.33 (d, J = 14.5 Hz, 3H), 4.25 (d, J = 14.2 Hz, 1H), 4.02–3.88 (m, 4H), 3.81–3.67 (br.s, 4H), 3.57 (d, J = 15.4, 4H), 2.92 (br.s 12H), 2.0–1.9 (m, 6H), 1.85–1.76 (m, 1.5H), 1.66–1.54 (m, 3.5H), 1.53–1.40 (m, 50H), 0.93–0.86 (m, 6H); ^{13}C NMR (100 MHz, $CDCl_3$) δ = 179.0 (C_q), 154.1 (C_q), 153.5 (C_q), 146.5 (C_q), 138.0 (C_q), 136.9 (C_q), 133.8 (C_q), 132.6 (C_q), 128.8 (CH), 126.8 (CH), 126.5 (CH), 125.0 (CH), 123.2 (CH), 74.0 (CH_2), 59.7 (CH_3), 34.2 (C_q), 31.4 (CH_3), 30.6 (CH_2), 29.6 (CH_2), 29.3 (CH_2), 26.3 (CH_2), 22.7 (CH_2), 14.1 (CH_3). HR-MS (ESI) m/z: = $[M+H]^+$ calcd. for $C_{92}H_{121}N_4O_6S_2$: 1441.8728 found 1441.8715.

NMR diffusion measurements

DOSY experiments were carried out on $CDCl_3$ and 5% v/v CD_3OD/$CDCl_3$ solutions of **DPT** at 300 K on a Bruker Avance III 400 Spectrometer using a stimulated echo sequence with bipolar gradients (STEbp). Because of the extensive signal overlapping and general broadness, the diffusion coefficient D of the diffusing species was calculated by applying a mono-exponential fitting of the decaying methoxy resonances at ca. 2.9 ppm. For each sample, 16 experiments were carried out, in which the gradient strength g was varied from 5 to 95% of the maximum gradient intensity (5.35 G mm^{-1}).

UV/Vis absorption spectroscopy

All spectroscopic measurements were performed on air-equilibrated CH_2Cl_2 (Uvasol) solutions at room temperature in 1 cm path length quartz cuvettes. UV/Vis spectra were recorded with a Cary 300 (Agilent) spectrophotometer. Spectrophotometric titrations were performed by adding a concentrated solution of the host to a more diluted solution of the guest. The apparent stability constants

of the pseudorotaxanes were obtained by fitting the absorbance changes with software Hyperquad,[27] according to a 1:1 binding model.

Electrochemical measurements

Cyclic voltammetric (CV) and differential pulse voltammetric (DPV) experiments were carried out in argon-purged CH_2Cl_2 (Sigma-Aldrich) with an Autolab 30 multipurpose instrument interfaced to a PC. The working electrode was a glassy carbon electrode (Amel, 0.07 cm^2), carefully polished with an alumina-water slurry on a felt surface, immediately before use. The counter electrode was a Pt wire, separated from the solution by a frit, an Ag wire was employed as a quasi-reference electrode and ferrocene was present as an internal standard[25] (see SI for details). Tetrabutylammonium tosylate (TBAOTs) was added in a 100-fold proportion with respect to the sample concentration, as supporting electrolyte. Cyclic voltammograms were obtained at scan rates varying from 50 to 1000 mV s^{-1}. Differential pulse voltammetries were performed with a scan rate of 20 mV s^{-1} (pulse height 75 mV). The IR compensation was used and every effort was made throughout the experiments in order to minimize the resistance of the solution. The electrochemical reversibility of the voltammetric wave of ferrocene was taken as an indicator of the absence of uncompensated resistance effects.

X-ray data collection and crystal structure determination

The crystal structure of **DPT** was determined by X-ray diffraction methods. Crystal data and experimental details for data collection and structure refinement are reported in Table S1. Intensity data and cell parameters were recorded on a Bruker ApexII diffractometer (MoKα radiation λ = 0.71073 Å) equipped with a CCD area detector and a graphite monochromator. The raw frame data were processed using the programs SAINT and SADABS.[28] The structure was solved by Direct Methods using the SIR97 program[29] and refined on F_o^2 by full-matrix least-squares procedures, using the SHELXL-2014/7 program[30] in the WinGX suite v.2014.1.[31] All non-hydrogen atoms were refined with anisotropic atomic displacements, except for some C atoms belonging to the alkyl chains. The carbon-bound H atoms were placed in calculated positions and refined isotropically using a riding model with C–H ranging from 0.95 to 0.99 Å and Uiso(H) set to 1.2–1.5 Ueq(C). The N-bound H atoms were found in the difference Fourier map and refined freely. The weighting schemes used in the last cycle of refinement was $w = 1/[\sigma^2 F_o^2 + (0.1344P)^2]$ where $P = (F_o^2 + 2F_c^2)/3$. The calculated molar mass, density and absorption coefficient include two disordered methanol molecules per unit cell which do not appear in the final files because of the refinement carried out with data subjected to SQUEEZE.[32] Deposition number 2083713 (for **DPT**) contains the supplementary crystallographic data for this paper. These data are provided free of charge by the joint Cambridge Crystallographic Data Centre and Fachinformationszentrum Karlsruhe Access Structures service www.ccdc.cam.ac.uk/structures.

Dynamic light scattering analysis

Dynamic light scattering (DLS) measurements were carried out using a Malvern Zetasizer Nano ZSP with a He–Ne laser source (l = 632.8 nm, power 35 mW), linearly polarized orthogonal to the scattering plane and an avalanche photodiode operating in single-photon counting to collect, in a self-beating mode, the scattered light with a measurement angle of 173° Backscatter (NIBS Default). A Malvern 4700 correlator was used to obtain the scattered intensity autocorrelation function, which, by means of the Laplace inversion method (CONTIN algorithm), gave the size distribution. Measurements were performed using a 1 cm path glass cuvette at 293 K. A solution of **DPT** was prepared dissolving 10 mg of **DPT** in 1 mL of $CHCl_3$. To this solution, increasing amounts of MeOH (twofold 50 μL) were added.[33]

Acknowledgements

The authors thank Centro Interdipartimentale di Misure of the University of Parma for NMR and MS measurements. This work was supported by the Italian Ministry of University and Research (PRIN 20173 L7 W8 K and FARE R16S9XXKX3). This work has been carried out within the COMP-HUB Initiative, funded by the "Departments of Excellence" program of the Italian Ministry for Education, University and Research (MIUR, 2018-2022). Open Access Funding provided by Universita di Bologna within the CRUI-CARE Agreement.

Conflict of Interest

The authors declare no conflict of interest.

Keywords: Anion binding · Calixarenes · Pseudorotaxanes · Semiempirical calculations · Viologen

[1] P. Neri, J. L. Sessler, M.-X. Wang, Eds., *Calixarenes and Beyond*, Springer International Publishing, **2016**.
[2] a) V. Balzani, A. Credi, M. Venturi, *Molecular Devices and Machines: Concepts and Perspectives for the Nanoworld*, Wiley-VCH, Weinheim, 2nd ed, **2008**.
[3] G. Cera, A. Arduini, A. Secchi, A. Credi, S. Silvi, *Chem. Rec.* **2021**, *21*, 1161–1181.
[4] a) A. Arduini, F. Calzavacca, A. Pochini, A. Secchi, *Chem. Eur. J.* **2003**, *9*, 793–799; b) A. Arduini, R. Bussolati, A. Credi, S. Monaco, A. Secchi, S. Silvi, M. Venturi, *Chem. Eur. J.* **2012**, *18*, 16203–16213; c) A. Arduini, R. Bussolati, A. Credi, A. Secchi, S. Silvi, M. Semeraro, M. Venturi, *J. Am. Chem. Soc.* **2013**, *135*, 9924–9930.
[5] M. Bazzoni, V. Zanichelli, L. Casimiro, C. Massera, A. Credi, A. Secchi, S. Silvi, A. Arduini, *Eur. J. Org. Chem.* **2019**, *21*, 3513–3524.
[6] G. Cera, M. Bazzoni, A. Arduini, A. Secchi, *Org. Lett.* **2020**, *22*, 3702–3705.
[7] a) F. A. Teixeira, P. M. Marcos, J. R. Ascenso, G. Brancatelli, N. Hickey, S. Geremia, *J. Org. Chem.* **2017**, *82*, 11383–11390; b) A. Nehra, S. Bandaru, D. S. Yarramala, C. Pulla Rao, *Chem. Eur. J.* **2016**, *22*, 8903–8914; c) N. Qureshi, D. S. Yufit, K. M. Steed, J. A. K. Howard, J. W. Steed, *CrystEngComm.* **2014**, *16*, 8413–8420; d) S. Moerkerke, S. Le Gac, F. Topić, K. Rissanen, I. Jabin, *Eur. J. Org. Chem.* **2013**, *2013*, 5315–5322; e) M. Hamon, M. Menand, S. Le Gac, M. Luhmer, V. Dalla, I. Jabin, *J. Org. Chem.* **2008**, *73*, 7067–7071.
[8] a) N. A. De Simone, S. Meninno, C. Talotta, C. Gaeta, P. Neri, A. Lattanzi, *J. Org. Chem.* **2018**, *83*, 10318–10325; b) M. Durmaz, A. Tataroglu, H. Yilmaz, A. Sirit, *Tetrahedron: Asymmetry* **2016**, *27*, 148–156; c) M. Durmaz, A. Sirit, *Supramol. Chem.* **2013**, *25*, 292–301.
[9] F. G. Bordwell, *Acc. Chem. Res.* **1988**, *21*, 456–463.
[10] a) M. Athar, M. Y. Lone, P. C. Jha, *Chem. Phys.* **2018**, *501*, 68–77; b) V. Blažek Bregović, N. Basarić, K. Mlinarić Majerski, *Coord. Chem. Rev.* **2015**, *295*, 80–124.
[11] D. E. Gómez, L. Fabbrizzi, M. Licchelli, E. Monzani, *Org. Biomol. Chem.* **2005**, *3*, 1495–1500.
[12] For a preliminary contribution, see: A. Arduini, R. Bussolati, C. Massera, A. Pochini, F. Rapaccioli, A. Secchi, F. Ugozzoli, *Supramol. Chem.* **2013**, *25*, 703–708.

[13] J. de Mendoza, M. Carramolino, F. Cuevas, P. M. Nieto, P. Prados, D. N. Reinhoudt, W. Verboom, R. Ungaro, A. Casnati, *Synthesis* **1994**, *1994*, 47–50.
[14] a) G. Luchini, D. M. H. Ascough, J. V. Alegre-Requena, V. Gouverneur, R. S. Paton, *Tetrahedron* **2019**, *75*, 697–702; b) S. J. Kim, M.-G. Jo, J. Y. Lee, B. H. Kim, *Org. Lett.* **2004**, *6*, 1963–1966.
[15] J. P. M. van Duynhoven, R. G. Janssen, W. Verboom, S. M. Franken, A. Casnati, A. Pochini, R. Ungaro, J. de Mendoza, P. M. Nieto, *J. Am. Chem. Soc.* **1994**, *116*, 5814–5822.
[16] a) R. Custelcean, *Chem. Commun.* **2013**, *49*, 2173–2182; b) R. Custelcean, *Chem. Soc. Rev.* **2010**, *39*, 3675–3685; c) Z. Zhang, P. R. Schreiner, *Chem. Soc. Rev.* **2009**, *38*, 1187–1198.
[17] a) H. M. Keizer, J. J. González, M. Segura, P. Prados, R. P. Sijbesma, E. W. Meijer, J. de Mendoza, *Chem. Eur. J.* **2005**, *11*, 4602–4608; b) A. M. Rincón, P. Prados, J. de Mendoza, *Eur. J. Org. Chem.* **2002**, *2002*, 640–644; c) J. J. González, R. Ferdani, E. Albertini, J. M. Blasco, A. Arduini, A. Pochini, P. Prados, J. de Mendoza, *Chem. Eur. J.* **2000**, *6*, 73–80.
[18] Tentative investigations of **DPT** in MeOD-d_4 and DMSO-d_6, failed due to the low solubility in these solvents.
[19] See e.g. a) C. S. Johnson, D. Wu, in *EMagRes*, American Cancer Society, **2011**; b) G. Pagès, V. Gilard, R. Martino, M. Malet-Martino, *Analyst* **2017**, *142*, 3771–3796.
[20] M. M. J. Smulders, M. M. L. Nieuwenhuizen, T. F. A. de Greef, P. van der Schoot, A. P. H. J. Schenning, E. W. Meijer, *Chem. Eur. J.* **2010**, *16*, 362–367.
[21] M. Korth, *J. Chem. Theory Comput.* **2010**, *6*, 3808–3816.
[22] J. J. P Stewart, *MOPAC2016*, Ver.: 21.145 W, Stewart Computational Chemistry, http://OpenMOPAC.net.
[23] It should be noted that such conformers distribution is opposite to that found for **TSA**-based pseudorotaxane with DOV. In this case, however, the computational studies evidenced that the flipping of one of the anisole ring of the host adopting the p*C* conformation generates a strain release of the whole intervowen structure, see ref. 6.
[24] A. Credi, S. Dumas, S. Silvi, M. Venturi, A. Arduini, A. Pochini, A. Secchi, *J. Org. Chem.* **2004**, *69*, 5881–5887.
[25] a) R. R. Gagne, C. A. Koval, G. C. Lisensky, *Inorg. Chem.* **1980**, *19*, 2854–2855; b) D. Dubois, G. Moninot, W. Kutner, M. T. Jones, K. M. Kadish, *J. Phys. Chem.* **1992**, *96*, 7137–7145; c) D. M. D'Alessandro, F. R. Keene, *Dalton Trans.* **2004**, 3950–3954.
[26] R. Zadmard, F. Hokmabadi, M. Reza Jalalia, A. Akbarzadeha, *RSC Adv.* **2020**, *10*, 32690–32722.
[27] P. Gans, A. Sabatini, A. Vacca, *Talanta* **1996**, *43*, 1739–1753.
[28] SADABS Bruker AXS; Madison, Wisconsin, USA, 2004; SAINT, Software Users Guide, Version 6.0; Bruker Analytical X-ray Systems, Madison, WI (1999). Sheldrick, G. M. SADABS v2.03: Area-Detector Absorption Correction. University of Göttingen, Germany, **1999**.
[29] A. Altomare, M. C. Burla, M. Camalli, G. L. Cascarano, C. Giacovazzo, A. Guagliardi, A. G. G. Moliterni, G. Polidori, R. Spagna, *J. Appl. Crystallogr.* **1999**, *32*, 115–119.
[30] G. M. Sheldrick, *Acta Crystallogr. Sect. A* **2008**, *A64*, 112–122.
[31] L. J. Farrugia, *J. Appl. Crystallogr.* **2012**, *45*, 849–854.
[32] P. v. d Sluis, A. L. Spek, *Acta Crystallogr. Sect. A* **1990**, *46*, 194–201.
[33] a) I. Pisagatti, L. Barbera, G. Gattuso, V. Villari, N. Micali, E. Fazio, F. Neri, M. F. Parisi, A. Notti, *New J. Chem.* **2019**, *43*, 7628–7635; b) F. Vita, A. Boccia, A. G. Marrani, R. Zanoni, F. Rossi, A. Arduini, A. Secchi, *Chem. Eur. J.* **2015**, *21*, 15428–15438.

Manuscript received: September 2, 2021
Revised manuscript received: September 6, 2021